Available online at www.sciencedirect.com
ScienceDirect
Journal of Environmental Sciences 20(2008) 907–914
JOURNAL OF ENVIRONMENTAL SCIENCES
ISSN 1001-0742
CN 11-2629/X
www.jesc.ac.cn

Effects of low temperature on aluminum(III) hydrolysis: Theoretical and experimental studies

XIAO Feng[1,*], ZHANG Baojie[2], LEE Chery[1]

1. Department of Civil Engineering, the Hong Kong University of Science and Technology, Clear Water Bay, Kowloon 999077, Hong Kong, China. E-mail: cexiao@ust.hk; fxiaoee@gmail.com
2. School of Municipal and Environmetal Engineering, Harbin Institute of Technology, Harbin 150001, China

Received 8 October 2007; revised 17 November 2007; accepted 23 November 2007

Abstract

In this study, the effects of low temperature on aluminum(III) (Al) hydrolysis were examined both theoretically and experimentally by constructing a solubility diagram for amorphous aluminum hydroxide ($Al(OH)_3$(am)) and a distribution diagram of hydrolyzed Al species. First, thermodynamic data of Al species at 4°C were calculated from that at 25°C. A well confirmed polymeric Al species, $AlO_4Al_{12}(OH)_{24}{}^{7+}$($Al_{13}$), was involved in building the diagrams and, correspondingly, the non-linear simultaneous equations with 13 degrees were resolved. Secondly, polarized Zeeman atomic absorption spectrophotometry (AAS), ^{27}Al nuclear magnetic resonance (NMR) spectroscopy, and ferron-based spectrophotometry were applied for constructing the practical diagrams. The results show that a decrease of temperature from 25 to 4°C caused the $Al(OH)_3$(am) boundary on the solubility diagram to shift toward the alkaline side by about 1.0 pH unit and the minimum solubility of $Al(OH)_3$(am) to reduce by 1.0 log unit. The distribution diagram indicates that the monomeric Al, Al_{13}, and solid-phase $Al(OH)_3$ were alternately the predominant species with the increase of pH value during Al hydrolysis. At 25°C, Al_{13} was the dominant species in a pH range of 4.0 to 4.5, whereas at 4°C, Al_{13} was the leading species in a pH range spaced from 4.5 to 6.3. The predominant species changed from the monomeric Al to the solid-phase $Al(OH)_3$ over the range of 1.8 pH units at 4°C in comparison with the range of 0.5 pH unit at 25°C.

Key words: low temperature; solubility diagram; distribution diagram; ^{27}Al NMR; Al_{13}

Introduction

Aluminum(III) (Al) hydrolysis is a chemical process in which $Al(H_2O)_6{}^{3+}$ reacts with, usually, water. It is common to omit the aquo ligands of the hydrolyzed species, for instance, $Al(H_2O)_6{}^{3+}$ becomes Al^{3+}. This practice is used in the remaining discussion. Unlike hydration, wherein molecules of water are added to a chemical compound without forming any other products, Al hydrolysis is applied to the reactions where the trivalent aluminum ions are converted to new ionic species and are precipitated. It is of great concern in the field of environmental, chemical, ocean, and earth engineering. For instance, in the field of coagulation via Al salts, two important mechanisms, adsorption-destabilization coagulation and sweep coagulation, are induced by the Al hydrolysis products formed *in situ* after dosing (Bottero *et al*., 1980; Sarpola *et al*., 2007; Van Benschoten and Edzwald, 1990). The hydrolysis of $Al(H_2O)_6{}^{3+}$ in water generates numerous species depending on ambient variables such as solution pH, temperature, and other co-existing anions, particularly $SO_4{}^{2-}$ and $CO_3{}^{2-}$ (Letterman and Asolekar, 1990; Sarpola *et al*., 2007; Ye *et al*., 2007). These hydrolyzed species can be generalized as monomers ($Al(OH)_n{}^{3-n}$, $n = 1 \sim 4$), polymers ($Al_m(OH)_n{}^{3-n}$), and solid-phase aggregates and/or precipitates (including aluminum hydroxide). In the last decades, advances in measuring technology have made it possible for researchers to capture some of these species. For instance, a kind of polymer, $AlO_4Al_{12}(OH)_{24}{}^{7+}$($Al_{13}$), has received much attention because its high positive charge is believed to be crucial for coagulation (Hu *et al*., 2006; Shi and Tang, 2006; Tang, 2000). Al_{13} has been successfully detected by ^{27}Al NMR and/or small angel X-ray diffraction (Bottero *et al*., 1980; Hu *et al*., 2006).

Environmental community attaches great importance on the Al hydrolysis. Unfortunately, and surprisingly, the effects of low temperature on the Al hydrolysis have not been given much focus in the literature and a clear understanding of it is lacking. Theoretically, a low temperature exerts great influence on an endothermic Al hydrolysis. However, people have a poor understanding about the population of the products at a cold environment. Van Benschoten and Edzwald (1990) observed that the $Al(OH)_3$ boundary on a $\log C_{Al}$-pH diagram shifted downwards and toward the alkaline side as temperature decreased. Nevertheless, as they pointed out, the $SO_4{}^{2-}$ in the coagulant $Al_2(SO_4)_3{\cdot}18H_2O$ (alum) they used can

* Corresponding author. E-mail: cexiao@ust.hk; fxiaoee@gmail.com.

precipitate with Al^{3+} to form $Al(OH)_{3-2x}(SO_4)_x$, which is believed to be the solid phase controlling solubility in the acidic pH range (Van Benschoten and Edzwald, 1990). The latest research also shows that the bivalent SO_4^{2-} is able to form polymers such as $(AlO_4Al_{12}(OH)_{25}(SO_4)_4)^{2-}$ with Al during Al hydrolysis (Sarpola *et al*., 2007). SO_4^{2-} is believed to promote the precipitation of hydroxide as well (Letterman and Asolekar, 1990). Therefore, studies using aluminum chloride are necessary to emphasize the effect of low temperature on Al hydrolysis. However, an examination of the features of chemical speciation using aluminum chloride at low temperatures is lacking in the literature and need to be conducted.

Furthermore, solubility of aluminum hydroxide refers to its ability to dissolve in water. For the trivalent aluminum ion, the solubility of its solid-phase precipitate $Al(OH)_3$ is affected by its numerous intermediate hydrolyzed products (Bottero *et al*., 1980). Conventionally, the effect of the products on solubility is illustrated by a solubility diagram of $\log C_{Al}$ versus pH. Because all of the lines on the diagram represent the concentrations that may exist at various pH values when in equilibrium with solid $Al(OH)_3$, it can be conceivable that any concentration of a particular species above the line in the diagram will be supersaturated with respect to $Al(OH)_3$ for that species (Johnson and Amirtharajah, 1982). The lines on the diagram show the maximum amount of species that can be added to the solution without precipitation. Moreover, the distribution diagram of hydrolyzed Al species illustrates the predominant domains of different species as functions of the concentration of aluminum and the solution pH. It provides a graphic representation of the individual species present at various pH values. One can see from the distribution diagram the pH range for a species that is being predominant, as well as the proportion of the species over the total C_{Al} (C_{Al_T}). Both the solubility and the distribution diagrams can be applied to predict and improve coagulation performance and minimize the amounts of residual Al (Amirtharajah and Mills, 1982; Amirtharajah and O'Melia, 1990; Kvech and Edwards, 2002). Through the development and application of the diagrams, this study theoretically and experimentally examined the effects of low temperature on Al hydrolysis.

1 Materials and methods

1.1 Al hydrolysis

The Al hydrolysis was conducted by titrating a 0.1 mol/L $AlCl_3{\cdot}6H_2O$ solution using 1.0 mol/L NaOH at a rate of 0.2 ml/min. The concentration of Al is selected as such by taking account of the popular and practical coagulant dosage in the water treatment plant, around 0.09 mol/L. The mixed solution was rapidly stirred continuously. All the solutions were prepared with a CO_2-free deionized distilled water (DDI). During the titration, N_2 was bubbled through the solution. The pH variation of the solution in the course of titration was measured by a pH meter (Model 420 A, Orion Research Inc., USA). The titration process was repeated at 4 and 25°C. The ratio of added C_{OH^-} to C_{Al_T} was termed as the hydrolysis ratio, marked as C_{OH^-}/C_{Al}. Particular attention was paid to the C_{OH^-}/C_{Al} (0.5, 1.0, 1.5, 2.0, 2.2, 2.5, 2.7, and 3.0). In the case of $C_{OH^-}/C_{Al} \geqslant 2.5$, the solution became seriously cloudy at the end of the titration, especially for the cold temperature, 4°C. The fresh aggregate in the $PACl_{2.5}$ sample was found to have a fractal dimension of 1.43 and contained –69 Al_{13} (Bottero *et al*., 1990). A very sticky gel was obtained when the solution (C_{OH^-}/C_{Al} ratio is 2.5) was filtrated using a 0.45-μm pore size membrane filter. The aggregate and precipitate in the solutions (C_{OH^-}/C_{Al} ratio $\geqslant$ 2.5) slowly settled after stirring was stopped. However, deposits were not found in other solutions with hydrolysis ratios smaller than 2.5, even though the solutions were also a little cloudy when C_{OH^-}/C_{Al} was up to 2.2.

1.2 Distribution of Al species in the process of Al hydrolysis

^{27}Al NMR (Model JNM EX-400, JEOL, Japan) was utilized to specify the hydrolyzed Al species. Al_{13} has a cage-like Keggin structure, that is, the center of Al_{13} is a tetrahedral $-AlO_4-$ which is surrounded by 12 other octahedrally coordinated Al ions (Bottero *et al*., 1990; Parker and Bertsch, 1992). The tetrahedrally coordinated Al ($-AlO_4-$) in Al_{13} can be reflected at the 62.5 ± 0.5 ppm resonance on a NMR spectrum with the assigned chemical shift of 0 ppm for Al^{3+} (Bottero *et al*., 1990; Parker and Bertsch, 1992). Furthermore, monomeric species including Al^{3+} can also be detected at 0 ppm. A predetermined quantity of $Al(OD)_4^-$ was used as the standard. $Al(OD)_4^-$ can be detected in the downfield peak at 80 ppm. Hence, in one spectrum, the integrated intensity of the peaks at 0 and 62.5 ppm was compared with that at 80 ppm to quantify, respectively, the monomeric Al and Al_{13} as the atomic Al. The difference between the C_{Al_T} and $C_{\text{monomeric Al + Al}_{13}}$ was designated as Al_u, which represents the undetectable Al species by ^{27}Al NMR, including large polymer species and/or solid-phase aluminum hydroxide. Because the solution became seriously turbid when C_{OH^-}/C_{Al} ratio $\geqslant$ 2.5, the expensive standard $Al(OD)_4^-$ was not used in its analysis using the liquid ^{27}Al NMR. For the measure of a sample of hydrolyzed Al species formed at 4°C, the reagents were pre-chilled, and the temperature of the sample in the NMR probe was controlled at 4°C.

Ferron-based spectrophotometry was also used to analyze the distribution of Al species during Al hydrolysis. The complex formed by ferron and Al species can be well detected by a UV spectrophotometer at 363 nm. The monomeric Al, Al_a, quickly completes its reaction with ferron within, often, 1 min. However, the reaction time is extended to 30 min for the reaction between polymeric Al (Al_b) and ferron, depending on the volume of the reactants. The difference between C_{Al_T} and $C_{Al_a + Al_b}$ is the unreactive part Al_c which refers to the large polymers and/or the solid-phase aluminum hydroxide. The composition of the ferron reagent and the procedure of the spectrophtometric analysis were introduced previously (Parker and Bertsch, 1992). The samples were diluted to 1×10^{-4} mol/L as

Al. Then 0.3 ml of the diluted sample was transferred to a cuvette located in the sample position of a UV-Visible spectrophotometer (Model Spectronic 3000, Milton Roy, USA). The assay time was recorded immediately after adding 0.95 ml ferron reagent (1.58 mol/L) into the cuvette so that ferron$_T$/Al$_T$ was about 50 in reference to the analysis (Parker and Bertsch, 1992). Meanwhile, the absorbance value was noted for every 20 s scan. The absorbance within 1 min was attributed to the monomeric Al, Al$_a$, while the absorbance with a time span of 1 to 30 min was ascribed to the polymeric Al, Al$_b$ (Parker and Bertsch, 1992). Note that the blank solution for the ferron method was a mixture of 0.3 ml DDI water and 0.95 ml ferron reagent.

1.3 Aluminum solubility

A pre-calculated amount of $AlCl_3$ stock solution (0.1 mol/L) was added into 1 L DDI water. When the solution was continuously stirred, its pH was adjusted by a predetermined volume of 0.1 mol/L NaOH and/or HNO_3. All the solutions were prepared using DDI water. During the adjustment, N_2 was bubbled through the solution to prevent the Al species from carbonation. The Al concentration in the final solution was 0.001 mol/L (pC_{Al} = 3). Samples were then collected, filtered by 0.20 μm membrane, and acidified to pH 1.0. The Al concentration was determined with AAS (Polarized Zeeman Atomic Absorption Spectrophotometer, Z-8200, Hitachi, Japan). Standard Al solution for a standard curve was prepared using aluminum metal (wire form, 99.99%). Tests of this section were repeated three times at both 4 and 25°C. And each time an Al-bearing solution was sampled three times by AAS. Finally, the mean value of the data was taken as Al concentration for a given setting.

2 Results and discussion

2.1 Solubility diagrams at different temperatures

2.1.1 Theoretical diagrams

Among many types of precipitate produced during the Al hydrolysis, the freshly formed amorphous aluminum hydroxide ($Al(OH)_3$(am)) is believed to be the predominant precipitate form in the water-treatment process and is usually selected as the controlling solid phase in the aluminum solubility diagram (Duan and Gregory, 2003; Johnson and Amirtharajah, 1982). The more stable crystalline hydroxide forms, such as gibbsite, require weeks to form and are of more concern in the study of river sediments or in the field of earth science (Amirtharajah and O'Melia, 1990). Steps for plotting the solubility diagram corresponding $Al(OH)_3$(am) in this study has been described previously (Benefield *et al*., 1982) and is briefly summarized in this section. The diagram was developed from purely thermodynamic equilibria.

For the hydrolyzed Al^{3+}, the formation of the hydrolyzed species can be illustrated by

$$m\mathrm{Al}^{3+} + n\mathrm{H_2O} \longrightarrow \mathrm{Al}_m(\mathrm{OH})_n^{(3m-n)+} + n\mathrm{H}^+ \quad (1)$$

The equilibrium constant K_{mn} of the formation reaction of $Al_m(OH)_n^{(3m-n)+}$ is

$$K_{mn} = \frac{C_{\mathrm{Al}_m(\mathrm{OH})_n^{(3m-n)+}} C_{\mathrm{H}^+}^n}{C_{\mathrm{Al}^{3+}}^m} \quad (2)$$

The logarithm of both sides of this equation results in

$$\log C_{\mathrm{Al}_m(\mathrm{OH})_n^{(3m-n)+}} = \log K_{mn} + n\mathrm{pH} + m\log C_{\mathrm{Al}^{3+}} \quad (3)$$

When aluminum hydroxide is formed, the hydrolyzed Al species is in equilibrium with the hydroxide. Hence, plotting the solubility diagram requires that the expressed Eq.(3) is concerned with the solubility product K_{so}. As shown in Eq.(4), the solubility of aluminum hydroxide is determined by the K_{so}, which is a constant at a given temperature.

$$\mathrm{Al(OH)_3(am)} \longrightarrow \mathrm{Al}^{3+} + 3\mathrm{OH}^- \quad (4)$$

Therefore,

$$\log K_{so} = \log C_{\mathrm{Al}^{3+}} + 3\log C_{\mathrm{OH}^-} \quad (5)$$

Because $C_{OH^-}=K_w/C_{H^+}$, where, K_w is the ion-product constant of water, Eq.(5) is changed to:

$$\log C_{\mathrm{Al}^{3+}} = \log K_{so} - 3\log K_w + 3\mathrm{pH} \quad (6)$$

Substituting for $\log C_{Al^{3+}}$ in Eq.(3) from Eq.(6) generates:

$$\log C_{\mathrm{Al}_m(\mathrm{OH})_n^{(3m-n)+}} = \log K_{mn} + m\log K_{so} - 3m\log K_w + (n-3)\mathrm{pH} \quad (7)$$

The overall equilibrium constants of the formation reactions of monomeric and polymeric Al species are listed in Table 1. The thermodynamic data of hydrolyzed Al species at 25°C were found from the literature (Baes and Mesmer, 1976; Benefield *et al*., 1982; Dempsey, 1987; Faust and Aly, 1998; Lydersen *et al*., 1990; Nordstrom and May, 1989). The Van't Hoff equation (Eq.(8)) was used to obtain equilibrium constants at 4°C based on the constants at 25°C. The standard enthalpy ΔH_r^o for the selected Al-hydrolyzed species can be found in the literature (Baes and Mesmer, 1976; Nordstrom and May, 1989).

$$\ln\frac{K_2}{K_1} = \int_{T_1}^{T_2} \frac{\Delta H_r^o}{RT^2}\mathrm{d}T \quad (8)$$

Based on Eqs.(7) and (8), the plotting lines for the selected Al-hydrolyzed species were developed and presented in Table 1. The solubility diagrams of $Al(OH)_3$(am) were then built (Fig.1). The interior portion of the diagrams designates the area in which precipitation of $Al(OH)_3$(am) may theoretically be expected. The boundary of $Al(OH)_3$(am) at any pH is actually the sum of the concentrations of all species present at that pH. If one species predominates at a particular pH, then its concentration will coincide closely with the $Al(OH)_3$(am) boundary. From Fig.1, all the plotting lines for the species shift toward the alkaline side with the decrease of temperature from 25 to 4°C which in agreement with Van Benschoten and

Table 1 Thermodynamic data of Al-species and plotting equations for solubility diagrams

	Species	25°C	4°C	25°C	4°C
Al^{3+}	$\log K_{so}$	–32.34	–33.18	$\log C_{Al^{3+}}$ = 9.66–3pH	$\log C_{Al^{3+}}$ = 10.98–3pH
$Al(OH)^{2+}$	$\log K_{11}$	–5.02	–5.38	$\log C_{Al(OH)^{2+}}$ = 4.64–2pH	$\log C_{Al(OH)^{2+}}$ = 6.60–2pH
$Al(OH)^{2+}$	$\log K_{12}$	–9.30	–11.30	$\log C_{Al(OH)_2^+}$ = 0.36–pH	$\log C_{Al(OH)_2^+}$ = –6.64
$Al(OH)_3$(aq)	$\log K_{13}$	–15.00	–18.62	$\log C_{Al(OH)_3(aq)}$ = –5.34	$\log C_{Al(OH)_3(aq)}$ = 0.68–pH
$Al(OH)_4^-$	$\log K_{14}$	–23.57	–26.31	$\log C_{Al(OH)_4^-}$ = pH–13.91	$\log C_{Al(OH)_4^-}$ = pH–14.33
$Al_2(OH)_2{}^{4+}$	$\log K_{22}$	–7.70	–8.73	$\log C_{Al_2(OH)_2^{4+}}$ = 11.62–4pH	$\log C_{Al_2(OH)_2^{4+}}$ = 15.23–4pH
$Al_3(OH)_4{}^{5+}$	$\log K_{34}$	–13.9	–15.86	$\log C_{Al_3(OH)_4^{5+}}$ = 15.08–5pH	$\log C_{Al_3(OH)_4^{5+}}$ = 27.07–5pH
$AlO_4Al_{12}(OH)_{24}(H_2O)_{12}{}^{7+}$	$\log K_{1324}$	–98.7	–114.18	$\log C_{Al_{13}}$ = 26.88–7pH	$\log C_{Al_{13}}$ = 41.53–7pH

Edzwald (1990). The shift results in part from the change in the ion-product constant of water (from $10^{-14.00}$ at 25°C to $10^{-14.78}$ at 4°C) and in part from the change in the equilibrium constants of the species (Table 1). The shift in equation line is more serious for species with a high polymerizing degree such as Al_{13}. Its line shifts almost two pH units when the temperature decreased from 25 to 4°C. As a result, the $Al(OH)_3$(am) boundary becomes rather narrow at low temperature.

Typically, the solubility of most solid solutes increases with temperature. However, $Al(OH)_3$(am) is well known for its typical amphoteric characteristic, resolving in either strong acid or alkali solution. For these amphoteric species, minimum solubility is the special term to describe their solubility. According to Fig.1, the minimum solubility of $Al(OH)_3$(am) decreases in the cold solution, a phenomenon that has been described elsewhere (Van Benschoten and Edzwald, 1990). $Al(OH)_3$(am) becomes less soluble at the low temperature only in a rather narrow pH range (Fig.1).

2.1.2 Practical solubility diagram

The practical solubility diagram shown in Fig.2 was developed according to the method introduced in Section 1.3. The practical diagram fits well with the theoretical one, especially at 25°C. At 4°C, there is a slight discrepancy between them in the pH range of 4.5–6.0, noted as a small amount of Al precipitated before the pH value predicted by the theoretical diagram. It is attributed to the aggregate of Al polymeric species such as $(Al_{13})_{69}$ (Bottero *et al*., 1990) that large enough to be captured by the 0.20 μm membrane. A regression line within the pH range of 6.3–7.0 on the practical diagram at 4°C gave a slope around –7, implying the presence of Al_{13}. The practical solubility diagram can be used for the rapid evaluation of total concentrations of all species present.

The observations from the theoretical and practical diagrams indicate that the reduction of temperature from 25 to 4°C caused a decrease in the minimum solubility of $Al(OH)_3$(am) by 1.0 log unit and a shift of the $Al(OH)_3$(am) boundary toward the alkaline side by around 1.0 pH unit. The $Al(OH)_3$(am) boundary in the acid range shifted significantly, which was primarily caused by the shift in the equation line of Al_{13}. Similar observations have been reported by Lydersen *et al*. (1990).

The solubility diagram may vary when other environmental factors, such as SO_4^{2-}, are considered (Bi *et al*., 2004; Letterman and Asolekar, 1990); however, it is not the focus of this study.

2.2 Effect of low temperature on the distribution of Al species

2.2.1 Theoretical interpretation

Currently, there are two models of formation of the Al-hydrolyzed species: Core-links model and cage-like Keggin-Al_{13} model (Bi *et al*., 2004). The first was proposed based on pH variation during potentiometric titration of Al-salt solutions. The model holds that the Al-hydrolyzed species are produced continuously from monomer to polymer by the bidimensional growth of hexametric ring units, e.g., $Al_6(OH)_{12}{}^{6+}$ (single ring) and

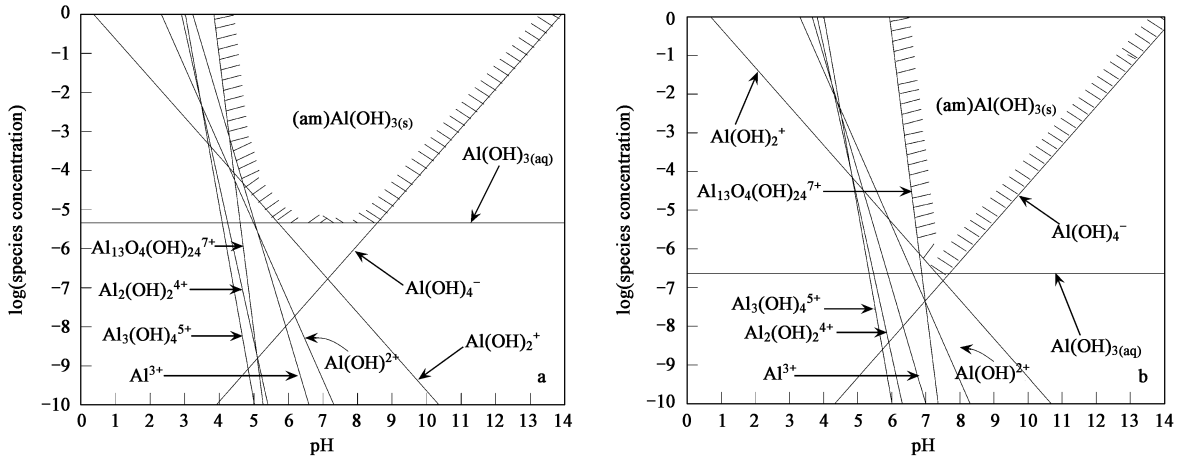

Fig. 1 Theoretical aluminum solubility diagram in equilibrium with amorphous $Al(OH)_3$. The thermodynamic data are from Table 1. (a) 25°C, (b) 4°C.

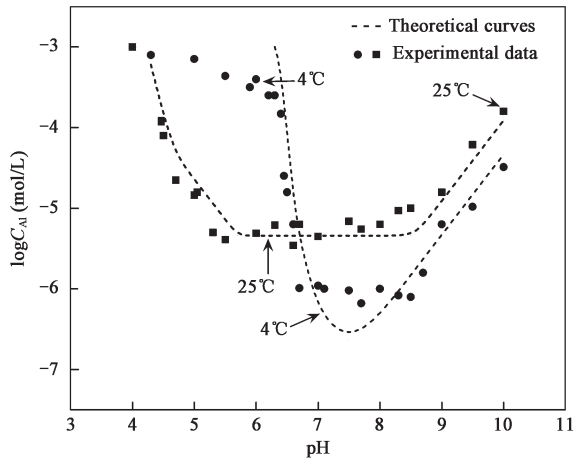

Fig. 2 Solubility data for dissolved aluminum in solutions of AlCl3. The curves are the theoretical solubility of aluminum in equilibrium with $Al(OH)_3$(am) (Fig.1).

$Al_{10}(OH)_{22}{}^{8+}$ (double rings). However, this model lacks the convincing experimental evidence supporting the existence of either the single ring or the double rings (Duan and Gregory, 2003). More researchers are think that monomers, dimers, Al_{13}, and larger hydrolyzed Al species including aggregates and aluminum hydroxide are the predominant species. This model is well supported by the existence of Al_{13} as detected by ^{27}Al NMR and/or small angle X-ray diffraction. The predominant positions of monomeric Al and Al_{13} among the soluble Al species have been confirmed as well (Zhang *et al*., 2004). Other polymers have been proposed, such as $Al_6(OH)_{12}{}^{6+}$, $Al_8(OH)_{20}{}^{4+}$, and $Al_{10}(OH)_{22}{}^{8+}$. Yet, many of them are not directly verified by experiments or are unlikely to be significant in practice (Duan and Gregory, 2003). Hence, in this study, Al_{13} was selected to represent large polymers ($Al_m(OH)_n{}^{3-n}$, $m > 6$) in constructing the distribution diagram of the hydrolyzed species. The steps of the construction are briefly described as follows.

From Eq.(2), the concentration of Al species can be expressed by $C_{Al^{3+}}$, pH, and formation equilibrium constant (Eq.(9)).

$$C_{Al_m(OH)_n^{(3m-n)+}} = \frac{K_{mn} \times C_{Al^{3+}}^m}{C_{H^+}^n} \tag{9}$$

The sum of the concentration of the selected species generates

$$\begin{aligned} &C_{Al^{3+}} + C_{Al(OH)^{2+}} + C_{Al(OH)^+} + C_{Al(OH)_3(aq)} + C_{Al(OH)_4^-} \\ &+C_{Al(OH)_2^{4+}} + C_{Al(OH)_4^{5+}} + C_{AlO_4Al_{12}(OH)_{24}^{7+}} = C_{Al_T} \end{aligned} \tag{10}$$

Before the formation of the solid-phase of $Al(OH)_3$, C_{Al_T} was the known quantity to calculate Eq.(10), which is a complex equation with thirteen degrees because of Al_{13}. When $Al(OH)_3$(am) is formed, Al^{3+} in the solution is in equilibrium with $Al(OH)_3$(am), and then its concentration is calculated from the solubility product of $Al(OH)_3$. The final concentration of each species in atomic Al is compared with C_{Al_T} to obtain the fractions of the species.

The results are provided in Fig.3, and only Al^{3+} in monomers and Al_{13} in polymers have considerable fractions. Al^{3+}, Al_{13}, and $Al(OH)_3$(am) are the predominant species alternately at both temperatures. A fall of temperature broadens the pH range for Al_{13} being the predominant species. As a consequence, the predominant species from Al^{3+} to $Al(OH)_3$(am) spaces almost 1.8 pH units apart at 4°C, while the change spaces around 0.5 pH unit at 25°C. Al_{13}, traditionally, is difficult to find its place on the distribution diagram, probably owing to the complicated and painstaking calculation of Eq.(10) with 13 degrees. If Al_{13} was not taken into account in the calculation of Eq.(10) and the construction of the diagram, monomers such as $Al(OH)^{2+}$ and $Al(OH)_2{}^+$ would be the leading species in the acid range. However, Al_{13} is the species that is remarkably present during Al hydrolysis, as reported in the literature (Zhang *et al*., 2004) and as shown in Fig.3 in this study.

2.2.2 Practical investigation

Figure 4 shows that there are three significant signals on the ^{27}Al-NMR spectra for all samples. As mentioned in Section 1.2, the peaks observed at 0, 63, and 80 ppm represent, respectively, the monomeric Al (Al_m), polymeric Al (Al_{13}), and $AlO_4{}^-$. The quantity of Al_m and Al_{13} were ascertained based on the integral intensities of the peak rather than the peak height. Controversial results may arise if the peak height was used in the quantification. The distribution of Al_m, Al_{13}, and Al_u are shown in Fig.5. From this figure, pH contributed directly to the population of hydrolyzed Al species. The monomeric Al predominated in high acid solutions and tied up about 97% of the total Al at the pH near 3.0. However, it ceased to predominate at pH 4.0 (25°C) or 4.5 (4°C). Al_{13} then became the predominant species in place of the monomeric Al. As shown in Fig.5, in the mildly acid solutions, Al_{13} was the most important polymeric species. Nevertheless, the pH range for Al_{13} being the predominant species was widened in the cold environment, as theoretically predicted by Fig.3. Duan and Gregory (2003) suggested that Al species maintained a positive charge at high pH and low temperature. Furthermore, in the neutral pH range, Al_u is the predominant species. Ozkan and Yekeler (2004) found that the solid-phase $Al(OH)_3$(am) is the main species at pH 4.5–9.0 at 25°C. From Fig.5, the pH range for Al_u being the predominant species shifted toward the alkaline side at the low temperature. As mentioned, Al_u represents the large polymer species and/or solid-phase aluminum hydroxide. Lydersen *et al*. (1990) reported that aluminum hydroxide became the dominant species at the rather alkaline side at 2°C in comparison with 25°C. A similar distribution of Al species at 25°C was developed by Bottero's group (Thomas *et al*., 1991).

In general, a good agreement exists between the theoretical distribution diagram and the practical one. However, the distribution of Al_{13} requires detailed clarification. At 25°C, the pH range for Al_{13} as the predominant species agrees well with the reported result (Hu *et al*., 2006). Nevertheless, at 4°C the maximum quantity of Al_{13} at pH

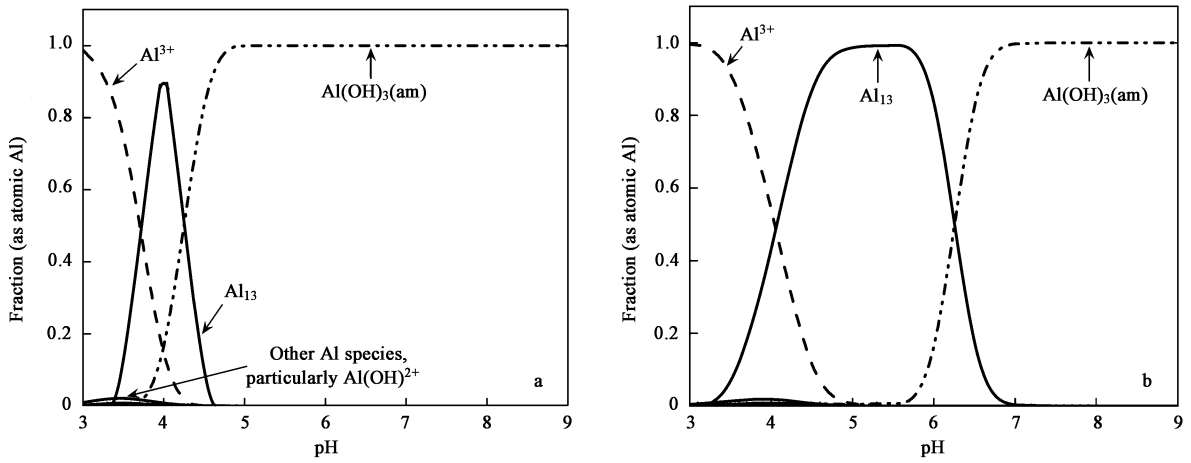

Fig. 3 Theoretical fractions of hydrolyzed Al products in equilibrium with amorphous $Al(OH)_3$(am) (C_{Al_T} = 0.1 mol/L). (a) 25°C; (b) 4°C.

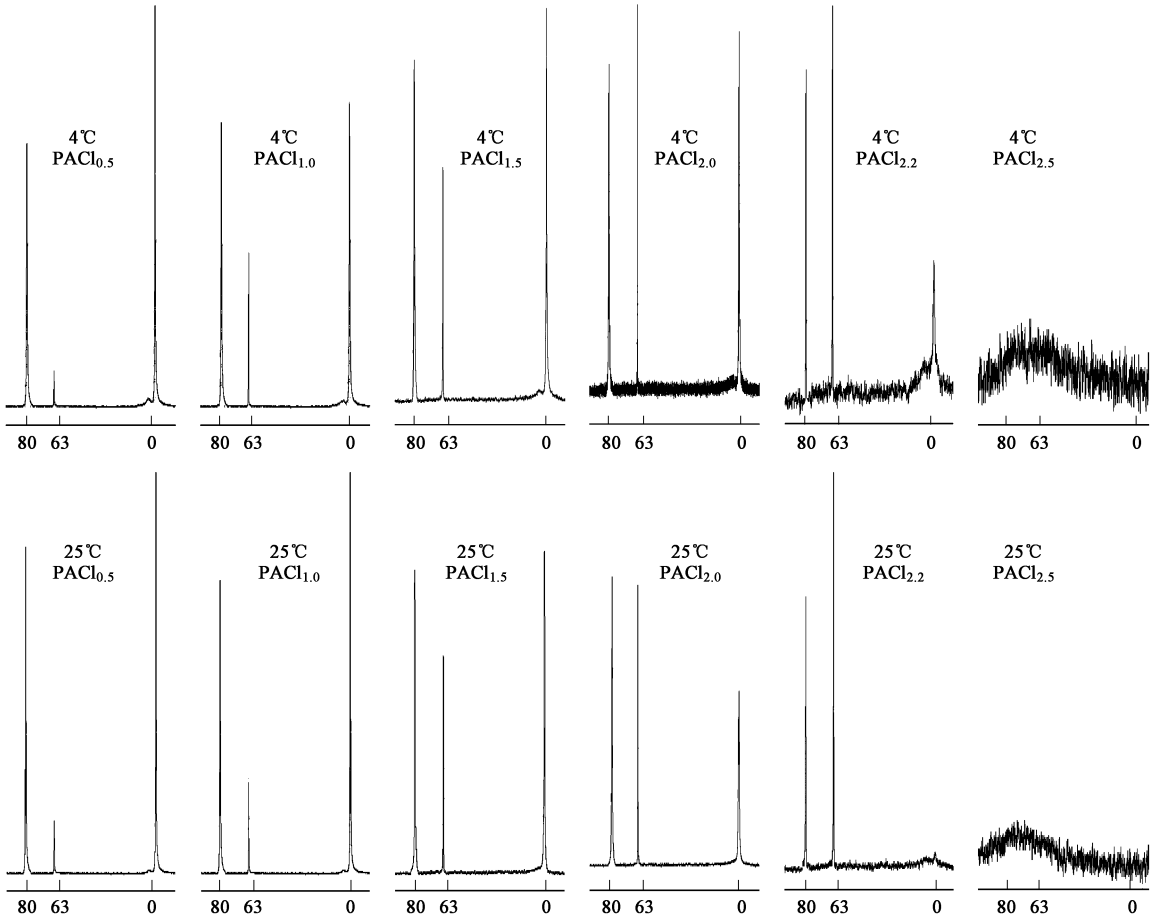

Fig. 4 ^{27}Al NMR spectra of $PACl_n$ samples.

5.0 was smaller than that at 25°C and the predicted one on Fig.3. Because aluminum hydroxide had not yet precipitated at pH 5.0 (Fig.2), the decreased content implies the existence of Al_{13} aggregates or other large polymers that are resistant to quantification by the liquid ^{27}Al NMR. In addition, such a group should account for 10%–20% of C_{Al_T} at 4°C. On the other hand, the phenomenon is not so noticeable at 25°C. Further, the serious fluctuation of signals on NMR spectra at 4°C implies that there are more noises for the liquid NMR to assay. It is then reasoned out that Al species at low temperature tend to hydrolyze into the intermediate species having a higher polymerizing degree than Al_{13} before the precipitation of $Al(OH)_3$(am), while at high temperature, the transformation from Al_{13} to $Al(OH)_3$(am) is much easier. In addition, the slight response near 3–4 ppm on the NMR spectra shown in Fig.4 signifies the dimeric Al (Hu *et al.*, 2006).

Figure 6 illustrates the distribution of hydrolyzed Al species analyzed by ferron spectrophotometry (Fig.7). Generally, the distribution of Al species in Fig.6 exhibits a similar behaviour as that in Fig.5. Monomeric Al (Al_a) declined rapidly with the increase of pH and reached

a minimum near the neutral pH value. Meanwhile, the polymeric Al increased at the expense of monomers and reached the maximum range at pH 4.3 (25°C) or pH 4.8 (4°C). As the pH further increased to the basic region, an inverse-V distribution of polymeric Al (Al_b) was observed because of the consumption of Al_b by forming the large polymers and/or solid-phase $Al(OH)_3$ (Fig.6). Al_b well represents Al_{13} (Hu *et al.*, 2006) in that Al_{13} is the predominant polymeric species (Fig.5), and thus the distribution of Al_b shown in Fig.6 bears a close parallel to that of Al_{13} presented in Fig.5. The pH range for polymeric species (Al_b) being the predominant on Fig.6 was wider at the low temperature. In contrast, at 25°C, a rapid fall in Al_b content was observed in the narrow pH range 4.5–5.0.

3 Conclusions

Aiming at better understanding the effects of low temperature on Al hydrolysis, a solubility diagram for $Al(OH)_3$(am) and a distribution diagram of Al species were developed from theoretical thermodynamic equilibria. Further, experiments and assays, polarized-Zeeman AAS, ^{27}Al nuclear magnetic resonance (NMR) spectroscopy, and ferron-based spectrophotometry were conducted to construct the practical diagrams and to assess the validity of the theoretical diagrams. In general, the theoretical diagram is in good agreement with the practical one. From what has been discussed, some points are stressed.

(1) When the temperature dropped from 25 to 4°C, the minimum solubility of $Al(OH)_3$(am) decreased by around 1.0 log unit, and the $Al(OH)_3$(am) boundary shifted toward the alkaline side by about 1.0 pH.

(2) The $Al(OH)_3$(am) boundary became rather narrow as a function of pH at the cold temperature.

(3) Monomeric species and the polymeric Al_{13} were the predominant species in the acid solution. $Al(OH)_3$(am) replaced them as the leading species in the solution whereby the solution was at a neutral to mildly alkaline pH.

(4) The mildly acid solution was critical for the forma-

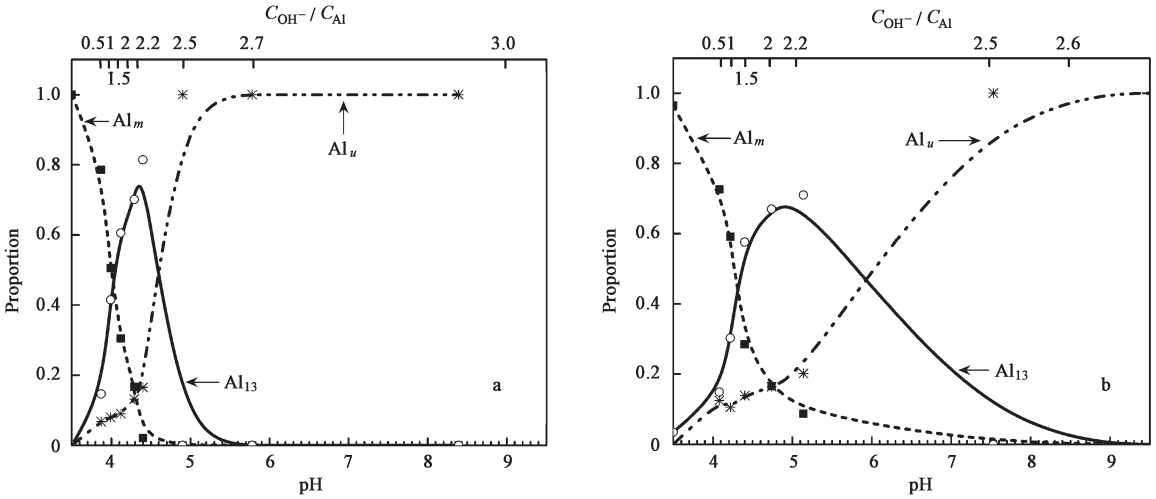

Fig. 5 Practical fractions of hydrolyzed Al products in equilibrium with amorphous $Al(OH)_3$(am) assayed by ^{27}Al NMR (C_{Al_T} = 0.1 mol/L). (a) 25°C; (b) 4°C.

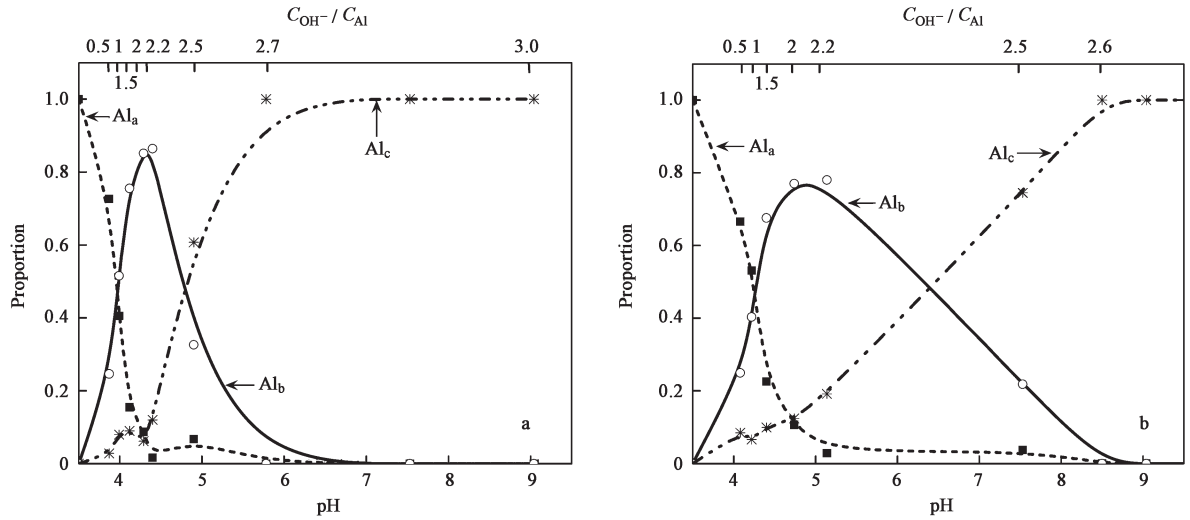

Fig. 6 Practical fractions of hydrolyzed Al species in equilibrium with amorphous $Al(OH)_3$(am) assayed by ferron method (C_{Al_T} = 0.1 mol/L). (a) 25°C; (b) 4°C.

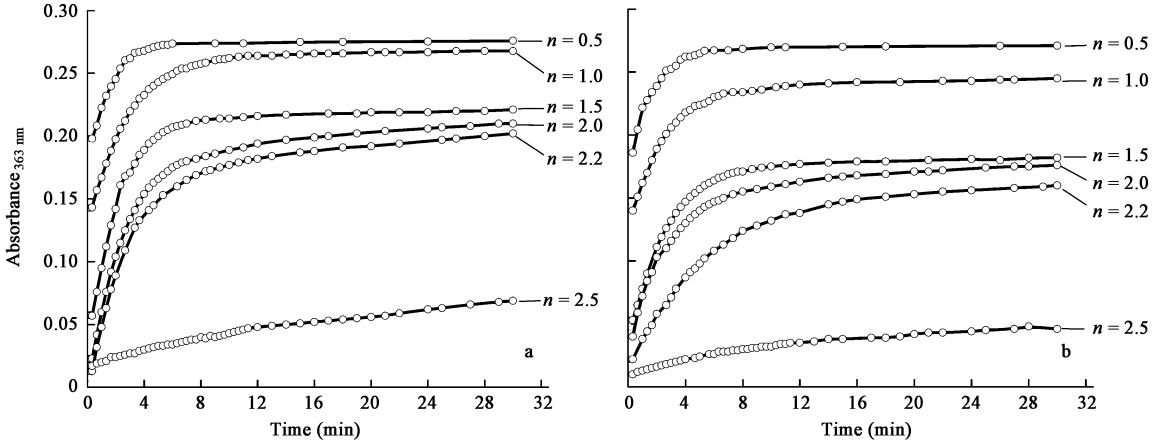

Fig. 7 Speciation of $PACl_n$ assayed by ferron-based spectrophotometry. (a) 25°C; (b) 4°C.

tion of Al_{13}. However, the pH range for Al_{13} being the dominant species was much wider at a cold environment. The predominant species changing from monomeric Al to $Al(OH)_3$(am) required 1.8 pH units at 4°C in comparison with the 0.5 pH unit at 25°C.

Acknowledgements

The kind advices from Dr. Chii Shang (HKUST) are greatly appreciated. And the authors express sincere appreciation to Mr. John Lee (technician in HKUST) for his the generous assistance in conducting the ^{27}Al-NMR assay. This work is primarily supported by the Promising Science and Technology Plan of the Hong Kong University of Science and Technology (No. HKUST/PST/06/EE).

References

Amirtharajah A, Mills K M, 1982. Rapid-mix design for mechanisms of alum coagulation. *J Am Water Works Assoc*, 74 (4): 210–216.

Amirtharajah A, O'Melia C R, 1990. Coagulation process: destabilization, mixing, and flocculation. In: Water Quality and Treatment (Pontius F. W., ed.). Denver, USA: McGraw-Hill, Inc. 269–367.

Baes C F, Mesmer R E, 1976. The Hydrolysis of Cations. New York, USA: John Wiley and Sons, Inc.

Benefield L D, Judkins J F, Weand B L, 1982. Process Chemistry for Water and Wastewater Treatment. New Jersey: Prentice-Hall, Inc. 281–299.

Bi S, Wang C, Cao Q, Zhang C, 2004. Studies on the mechanism of hydrolysis and polymerization of aluminum salts in aqueous solution: correlations between the "Core-links" model and "Cage-like" Keggin-Al_{13} model. *Coordination Chemistry Reviews*, 248: 441–445.

Bottero J Y, Tchoubar D, Cases J M, Fiessinger F, 1980. Studies of hydrolyzed aluminum chloride solutions. 1. Nature of aluminum species and composition of aqueous solutions. *J Phys Chem*, 84: 2933–2939.

Bottero J Y, Tchoubar D, Axelos M, Quienne P, Fiessinger F, 1990. Flocculation of silica colloids with hydroxy aluminum polycations: relation between floc structure and aggregation mechanisms. *Langmuir*, 6: 596–602.

Dempsey B A, 1987. Chemistry of Coagulats. Proceedings of Seminar on Influence of Coagulation on the Selection, Operation and Performance of Water Treatment Facilities. American Water Works Association. Denver: 19–30.

Duan J, Gregory J, 2003. Coagulation by hydrolyzing metal salts. *Advances in Colloid Interface Sci*, 100-102: 475–502.

Faust S D, Aly O M, 1998. Chemistry of Water Treatment. Michigan: Ann Arbor Press, Inc.

Hu C, Liu H J, Qu J H, Wang D S, Ru J, 2006. Coagulation behavior of aluminum salts in eutrophic water: significance of Al_{13} species and pH control. *Environ Sci Technol*, 40: 325–331.

Johnson P N, Amirtharajah A, 1982. Ferric chloride and alum as single and dual coagulants. *J Am Water Works Assoc*, 75: 232–239.

Kang L S, Cleasby J L, 1995. Temperature effects on flocculation kinetics using Fe(III) coagulant. *J Envir Engrg Div ASCE*, 121(12): 893–901.

Kvech S, Edwards M, 2002. Solubility controls on aluminum in drinking water at relatively low and high pH. *Water Res*, 36(17): 4356–4368.

Letterman R D, Asolekar S R, 1990. Surface ionization of polynuclear species in Al(III) hydrolysis–1. titration results. *Water Res*, 24(8): 931–939.

Licsko I, 2004. Coagulation mechanisms: nano- and microprocesses. *Water Sci Technol*, 50(12): 193–200.

Lydersen E, Salbu B, Poleo A B S, Muniz I P, 1990. The influences of temperature on aqueous aluminum chemistry. *Water Air and Soil Poll*, 51: 203–215.

Nordstrom D K, May H M, 1989. Aqueous equilibrium data for mononuclear aluminum species. In: The Environmental Chemistry of Aluminum (Sposito G., ed.). Boca Raton, Florida, USA: CRC Press. 29–55.

Ozkan A, Yekeler M, 2004. Coagulation and flocculation characteristics of celestite with different inorganic salts and polymers. *Chemical Engineering and Process*, 43: 873–879.

Parker D R, Bertsch P M, 1992. Identification and quantification of the "Al_{13}" tridecameric polycation using ferron. *Environ Sci Technol*, 26: 908–914.

Sarpola A, Hellman H, Hietapelto V, Jalonen J, Rämö J, Saukkoriipi J, 2007. Hydrolysis products of water treatment chemical aluminum sulfate octadecahydrate by electrospray ionization mass spectrometry. *Polyhedron*, 26: 2851–2858.

Shi B Y, Tang H X, 2006. Preparation and characterization of organic polymer modified composite polyaluminum chloride. *J Environ Sci*, 18(2): 214–220.

Tang H X, 2000. Application of surface coordination principle and modeling on aquatic micro-interfacial processes impacting the water quality. *Acta Scientiae Circumstantiae*, 20(1): 1–9.

Thomas F, Maslon A, Bottero J Y, Rouiller J, Genévrler F, Boudot D, 1991. Aluminum(III) speciation with acetate and oxalate: A potentiometric and ^{27}Al NMR study. *Environ Sci Technol*, 25(9): 1553–1559.

Van Benschoten J E, Edzwald J K, 1990. Chemical aspects of coagulation using aluminum salts–1. hydrolytic reactions of alum and polyaluminum chloride. *Water Res*, 24(12): 1519–1526.

Ye C, Wang D, Shi B, Yu J, Qu J, Edwards M, Tang H, 2007. Alkalinity effect of coagulation with polyaluminum chlorides: Role of electrostatic patch. *Colloids Surf* A: *Physicochem Eng Aspects*, 294: 163–173.

Zhang P, Hahn H H, Hoffmann E, Zeng G, 2004. Influence of some additives to aluminum species distribution in aluminum coagulants. *Chemosphere*, 57: 1489–1494.